A photometric study of the solar aureole under various weather conditions

By BO RYDGREN, *Stazione Astrofisica Svedese, Anacapri, Italy*

(Manuscript received October 5, 1966)

ABSTRACT

By means of a coronagraph and a visual skyphotometer which is based upon coronagraph principles, the intensity of the solar aureole in the interval 4′–66′ from the sun limb has been studied. The results show that there is a good correlation between the type of prevailing air mass and the characteristics of the measured intensity. The intensity variation with time and height is studied and discussed.

Introduction

Even during cloudless days with very clear air there is around the sun a more or less bright ring, which is formed by the scattering of sun light in the atmosphere. The particles that cause this scattering process consist partly of air molecules and partly of the specific content of the atmosphere: water-drops, ice-crystals, salt-particles, sand, etc.

The appearance of the ring (the solar aureole depends mainly on the number, structure, radii and distribution of the scattered particles. The wave-length of the scattered light is also important and must be considered. The intensity ratio of the aureole to the intensity of the sun centre is in general of the order 10^{-2}–10^{-6}. Even the gradient of the radiance shows a clear variation with the air mass content when observed at the same sun-height.

Meteorologists have always been interested in finding an objective way to classify the air masses in order to deduce their origin and thus indirectly their physical properties. The method reported here provides a possible way to determine qualitatively the state of the atmosphere.

The main parameters examined in this study are the aureole intensity close to the sun and the radial gradient of the scattered light counted from the sun limb. These two parameters show a great variation with the prevailing weather type. Even the variation of the radiance with time and height at a constant distance from the sun centre has been investigated.

Similar studies have been performed previously by means of special photometers, e.g. in U.S.A. and Germany (G. A. Newkirk 1956; F. Volz, 1954). The difficulties connected with the measuring procedure have always been to examine the sky close to the limb, where the sensitivity of the phenomena is maximal. These difficulties of course arise from the low intensity of the scattered light compared with that of the sun, which normally, as mentioned, exceeds the scattering effect up to 10^6 times.

A suitable instrument to overcome most of these problems is the Lyot-coronagraph, with which the sun can be hidden behind occulting disks of different extension, permitting only the scattered light at determined distances from the limb to be studied. A coronagraph is, however, too complicated for use in field studies, in which it is important to measure e.g. the variation of the intensity with height. Therefore a more practical instrument for this part of the work has been used in this study, namely the VSP-AI-photometer constructed by J. W. Evans (1948) at the High Altitude Observatory of Harvard University, U.S.A.

The measurements were made mainly during the spring 1963 at the Swedish Astrophysical Observatory, Anacapri, Italy. By means of the bigger coronagraph of this station, the sky-photometer was calibrated during the autumn and winter of 1959 and 1962. The calibration curve was checked before the observation period started in 1965.

The instruments and their principles

The bigger coronagraph of the Swedish Astrophysical Observatory was constructed and built by Y. Öhman, E. Aulin & F. Thorlin, according

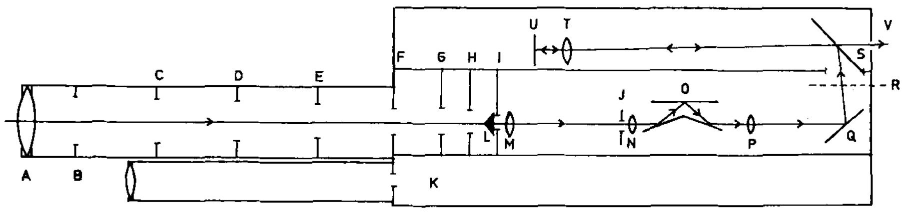

Fig. 1. Schematic diagram of the coronagraph at the Swedish Astrophysical Observatory, Anacapri, Italy. A, Objective; B–J, Diaphragm; K, Smaller coronagraph; L, Occulting disk; M, Field lens; N, Collimating lens; O, Dove-prism for turning the image; P, Collimating lens; Q/S, Mirror; R, Focal-plane for *P* and *T* (variable slit); T, Autocollimation lens; U, Grating; V, Photometer [Fig. 2]; →– One ray from the sun aureole.

to Lyot's principles (Y. Öhman, 1955). The instrument has an aperture of 12 cm and a focal length of 150 cm (Fig. 1). The objective of the spectrograph, built on the principle of autocollimation, has a focal length of 80 cm and a grating, ruled by M. Siegbahn, with 576 lines per mm, which gives a dispersion of 21 Å per mm in the first order.

For measuring the sky brightness a visual photometer, designed by Y. Öhman, has been used (Fig. 2). In the focal plane *A* of the spectrograph there is a metal plate *B* with a large "window" *C*, in which the spectrum outside the limb could be observed, and there is also a slit *D* with a variable width for direct measurement of the continuous spectrum of the sun. In front of the plate *B* neutral filters T_1–T_4 of different transmission powers could be placed. These filters have been calibrated carefully by F. Lindgren (1954). The properties of the calibrated filters used in this study are given in the following table:

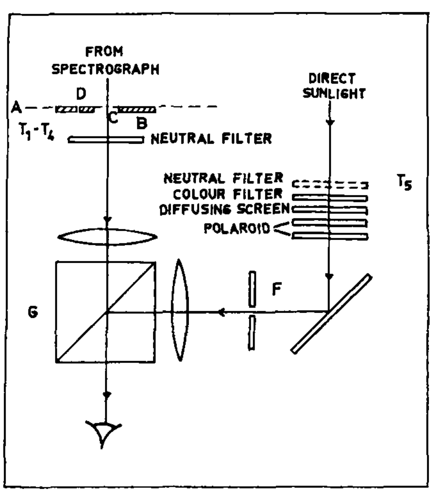

Fig. 2. Schematic diagram of the Öhman visual photometer (4).

In the side-tube, used for observing the direct sunlight, there is a green filter, a diffusing screen and a neutral filter T_5, which reduce the incoming sunlight to a suitable order. The most important part of the photometer is a pair of polaroid filters; by means of rotating these mutually through a certain angle it is possible to obtain the same intensity of the two images *F* and *D*, which are observed in the prism *G* (Fig. 2).

When measuring the intensity of the scattered light around the sun, *F* is viewed close to *D* and their widths are made equal. (During the calibration procedure *D* was held at a distance $\sim 5'$ from the sun limb). By turning the analyser an angle v_1, *F* is given the same intensity as *D*. v_1 is computed from a zero-point at which the polaroids are crossed and the measurements are repeated at least four times on each side of this zero-point.

The intensity of the sun aureole at the selected distance when no filter is used is equal to

$$i_s \sin^2 v_1,$$

where i_s is the intensity of the direct incoming sunlight.

The same procedure is then immediately repeated with the sun centre in D.

The intensity received can now be written

$$i_s \sin^2 v_2.$$

As mentioned before, the directly incoming sunlight must be reduced by using filters. If i_c is the sun-centre intensity and t_3 is a suitable transmission factor according to the prevailing air conditions

$$i_s \sin^2 v_2 = t_3 i_c. \quad (1)$$

Table 1. *Calculated and measured transmission powers for neutral filters (5)*

Filter	Thickness, mm	Wavelength, Å	Transmission-factor t Calculated	Measured
T_1 NG5	1.865	5303	0.318	0.303
T_2 NG4	2.085	5303	0.126	0.124
T_3 NG3	2.250	5303	0.0085	0.0168
T_4 NG4 + NG9	2.085 + 1.150	5303	0.00372	0.00337
T_5 NG3	2.050	5303	0.0129	0.0150

In the same way the intensity of the aureole at a certain distance i_H is reduced by using one of the filters T_1–T_4, and the filter T_5 is placed in front of the polaroids in order to obtain a sufficiently great measuring interval on the analyser. We get

$$t_5\, i_s \sin^2 v_1 = t_1\, i_H, \tag{2}$$

and from (1) to (2)

$$i_H = \frac{t_3 t_5 \sin^2 v_1}{t_2 \sin^2 v_2} \cdot i_c. \tag{3}$$

To obtain a good calibration of the VSP–AI-skyphotometer every measurement with the bigger coronagraph was compared with a simultaneous observation of the sky brightness with the portable skyphotometer. This instrument, which also works according to coronagraph principles, is described in Fig. 3. It has an aperture A of 3 mm and is equipped with an external occulting disk B which could be varied in radius between 1.25–5 $R_\odot$ in order to study the intensity of scattered light of distances from 4′–66′ from the sun limb. The distance A–B is 100 cm. Behind A is placed an objective C with a focal length of 25 cm and an eye piece D (f = 10 cm). The incoming rays are reflected in a black glass mirror E. There is also in the focal plane of D a second occulting disk F, which acts as a comparison surface. The surface F is painted diffusing white and the direct sunlight illuminates it after having passed an optical wedge G. When the observer looks into the aperture diaphragm H (which is slightly smaller than the image of the bright edge of A in order to prevent the diffracted light from edge A from entering the observer's eye) he sees F surrounded by an image of the sky. The extent of this image depends on the selected radius of the occulting disk B. For B the following radii were used: 1.25, 1.5, 2, 2.5, 3, 3.5, 4, 4.5 and $5 \times R_\odot$.

From the known density of the optical wedge the sky brightness i_H then is obtained for the average brightness of the sun i_s (3).

$$i_H = i_s \cdot \frac{\varphi^2 \cdot \cos\beta \cdot r_1}{t_a \cdot r_E} \cdot t_W, \tag{4}$$

where i_H = brightness of sky;
i_s = brightness of sun;
φ = angular radius of sun (0.0047 radians);
β = angle of incidence of sunlight on F;
t_a = transmission of C and D;
t_W = transmission of the wedge at balanc;
r_1 = diffuse reflecting power of white surface on F;
r_E = reflecting power of mirror E.

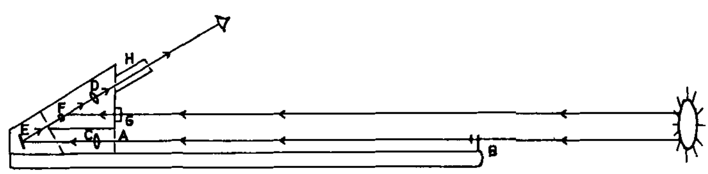

Fig. 3. Schematic diagram of the VSP–AI sky photometer (3). A, Aperture; B, Occulting disk; C, Objective; D, Eye piece; E, Black mirror (partly reflecting); F, Comparison surface; G, Optical wedge; H, Aperture diaphragm.

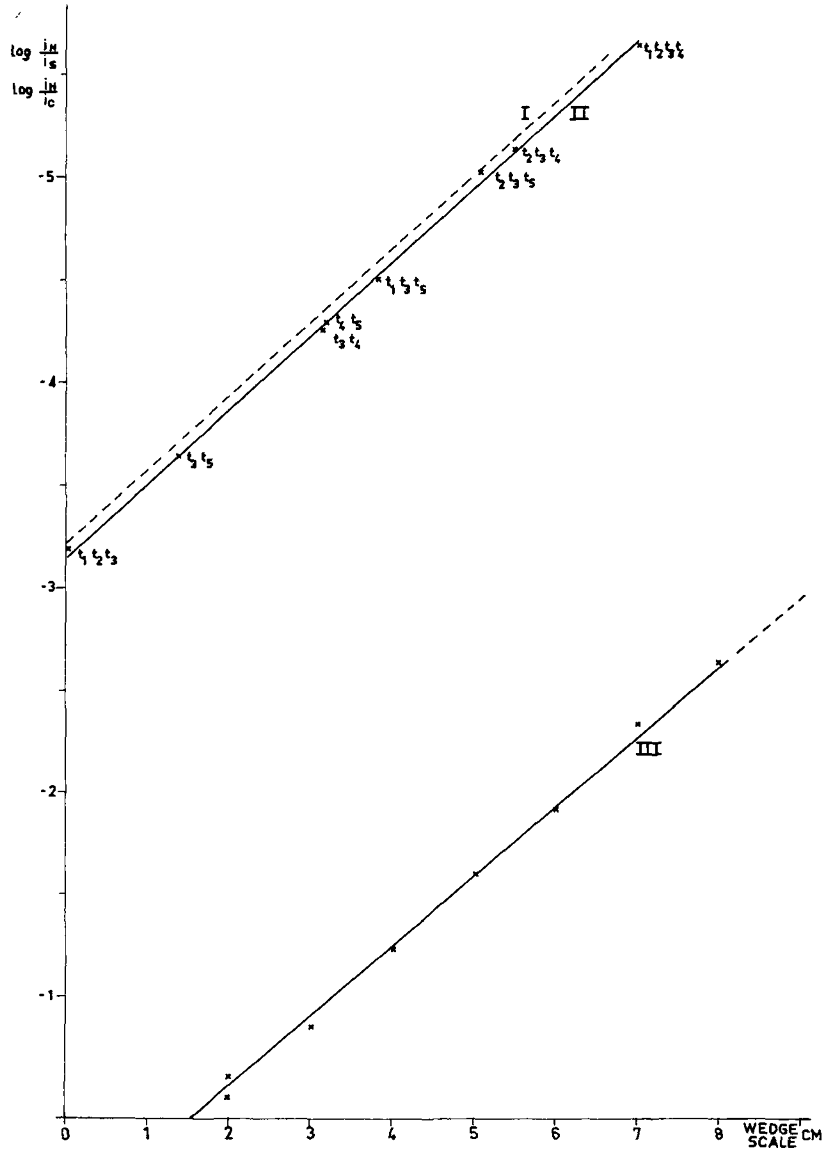

Fig. 4. Calibration (I and II) and comparison (III) curves for the sky photometer.

From simultaneous observations during 1959 and 1962 with the two instruments, an acceptable comparison curve was obtained for the sky photometer (curve 1, Fig. 4). This curve was checked in 1965 under various sky conditions. To be certain that no severe errors had been included, a second calibration curve was calculated in the following manner: The sun disk was displaced in relation to the diffusing screen *F*, and the two images were made equal in intensity by using different combinations of the calibrated neutral filters T_1–T_5 in front of the aperture *A* (without the occulting disk). The wedge as before reduced the intensity of the screen *R* (curve II, Fig. 4).

As the mean surface intensity of the sun for $\lambda = 5062$ Å (a green filter Wratten No. 58 was used in the aperture diaphragm *H*) is equal to the observed intensity at 0.8 $R_\odot$ (6), the calculated intensity i_s for all the sun surface is 75%

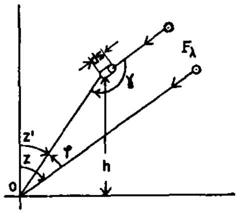

Fig. 5. Parameters used in the theoretical discussion (2).

of the centre intensity i_c at this wavelength. This means that there will be a small difference between the two methods of calibration depending on the difference in comparison intensity. This difference can be expressed as

$$\log \frac{i_s}{i_c} = \log 0.75 = -0.125 \cdot \qquad (5)$$

This is in good agreement with the mutual parallel displacement between the two calibration curves I and II (Fig. 4). The slope of the curves has been checked through a photometric calibration of the wedge by means of a mirror galvanometer, type AOH, and in green light (curve III, Fig. 4) by using an ordinary lamp, the intensity of which was compared with that of the sun's surface. The three curves are, as can be seen from Fig. 4, acceptably parallel with each other.

From curves I and II we obtain the following linear functions

$$\text{curve I: } \log \frac{i_H}{i_c} = -(0.36\,p + 3.22), \qquad (6)$$

$$\text{curve II: } \log \frac{i_H}{i_s} = -(0.36\,p + 3.14), \qquad (7)$$

where p is the scale-number of the wedge.

Thus $\log i_s/i_c = -0.08$, which should be compared with the calculated theoretical value in (5).

Theory

We regard the sun as a point source (G. A. Newkirk) with the zenith distance z (Fig. 5). The flux with wave length λ at the top of the atmosphere is F_λ. A unit cross-section volume element of length ds and at altitude h is assumed to scatter an amount of illuminance dE_λ in the direction φ, counted from the sun centre

$$dE_\lambda(z', \varphi, h) = F'_\lambda f_\lambda(\varphi, h)\, ds, \qquad (8)$$

where z' = zenith distance to the scattering volume;
$z - z'$ = φ;
h = height above zero level of the scattering volume;
F'_λ = flux of the solar radiation at (z', h)
f_λ = $(\varphi, h$ = volume scattering function for the wavelength;
λ at (φ, h).

Moreover, we have the fundamental transmission equation

$$F'_\lambda = F_\lambda e^{-\sigma_\lambda(h) \sec z}, \qquad (9)$$

where σ_λ is the optical depth at height h.

Integrating over all elements along the sight line at an angular distance φ from the sun, one obtains

$$E_\lambda(z, \varphi) = e^{-\sigma_\lambda(0) \sec z} \sec z \int_0^\infty F_\lambda f_\lambda(\varphi, h)\, dh. \qquad (10)$$

The ratio of the sky luminance $B_\lambda(z, \varphi)$ to the average luminance $B_\lambda(0)$ of the solar disk is then

$$\frac{B_\lambda(z, \varphi)}{B_\lambda(o)} = w_0 \sec z \int_0^\infty F_\lambda(\varphi, h)\, dh = \frac{i_H}{i_s}, \qquad (11)$$

where w_0 is the solid angle subtended by the sun.

The expression (11) can now be applied to two different cases of scattering:

1. With the assumption of only Rayleigh scattering for unpolarized light, f_λ can be expressed as

$$f_\lambda(\varphi) = \frac{2\pi^2}{h\lambda^4}(\mu_\lambda - 1)^2 (1 + \cos^2 \varphi), \qquad (12)$$

where n is the specific number of molecules and μ_λ the refractive index at NTP.

2. In addition to the molecular Rayleigh scattering there is another scattering process, depending on the particle spectrum of the atmosphere, that is more important for this study. G. Mie (1908) has calculated the scattering coefficient for the general case to be

$$f_{\lambda, n}(\gamma, \alpha) = \frac{\lambda^2}{8\pi^2}\{i_1(\gamma, n, \alpha) + i_2(\gamma, n, \alpha)\} N(\alpha, n), \qquad (13)$$

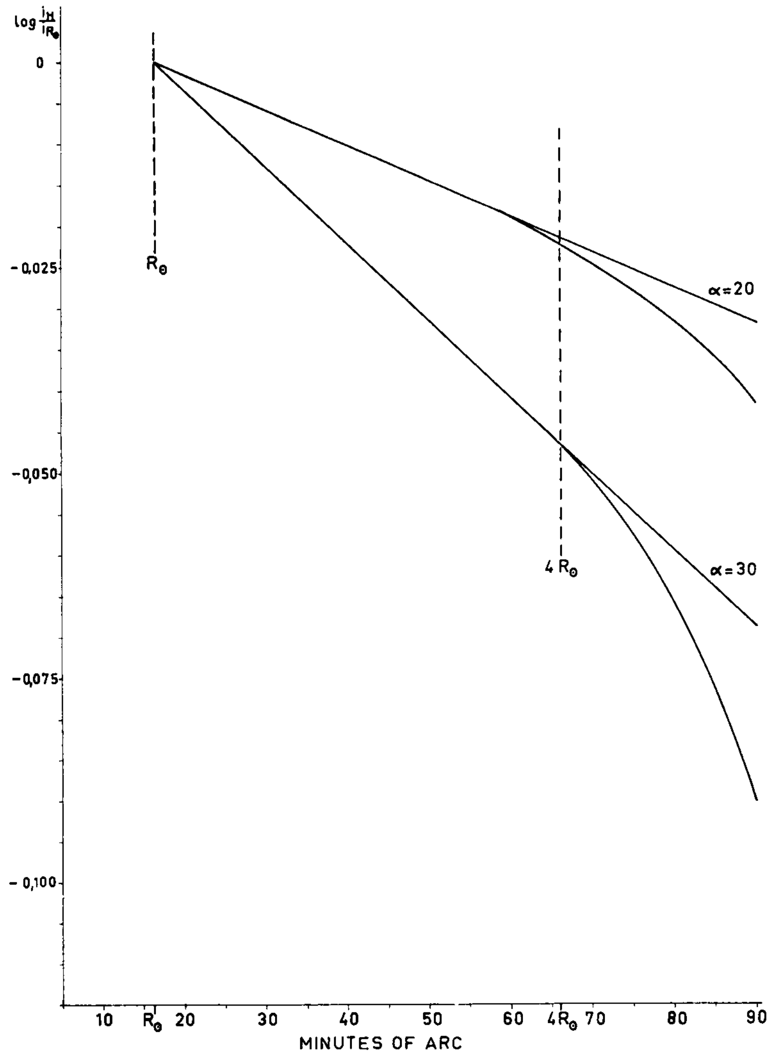

Fig. 6. Angular distribution of the relative intensity of the light scattered by water droplets (2).

where n = refractive index of the particle;
γ = 180° $-\varphi$ (scattering angle);
α = 2 Π a/λ (size parameter);
$N(\alpha, n)$ = number of particles with size parameter α (a = drop radius) and refractive index n;
i_1 and i_2 = quantities proportional to the plane polarized components.

According to Penndorf's calculations (8), (9) the function i_1 and i_2 for $n = 1.33$ (water), for $0.1 \leqslant \alpha \leqslant 30.0$ and for $0° \leqslant \gamma \leqslant 180°$ are available in a tabular form. Fig. 6 shows the angular distribution of the scattered radiation for different values of the size parameter for an atmosphere containing only water drops. As we can see from this diagram, it is possible to substitute the curves with their asymptotes in the intervals of interest, namely up to about 60′. It is observed, however, that there is no further agreement between the theoretical curves in Fig. 6 and the angular distribution of the studied aureoles (Fig. 7), which in our case are caused mainly by mixtures of dust-, ice- and water particles.

It is thus obvious that the function i_H/i_C = $= f(r)$, or $i_H/i_s = f(r)$, is exponential up to

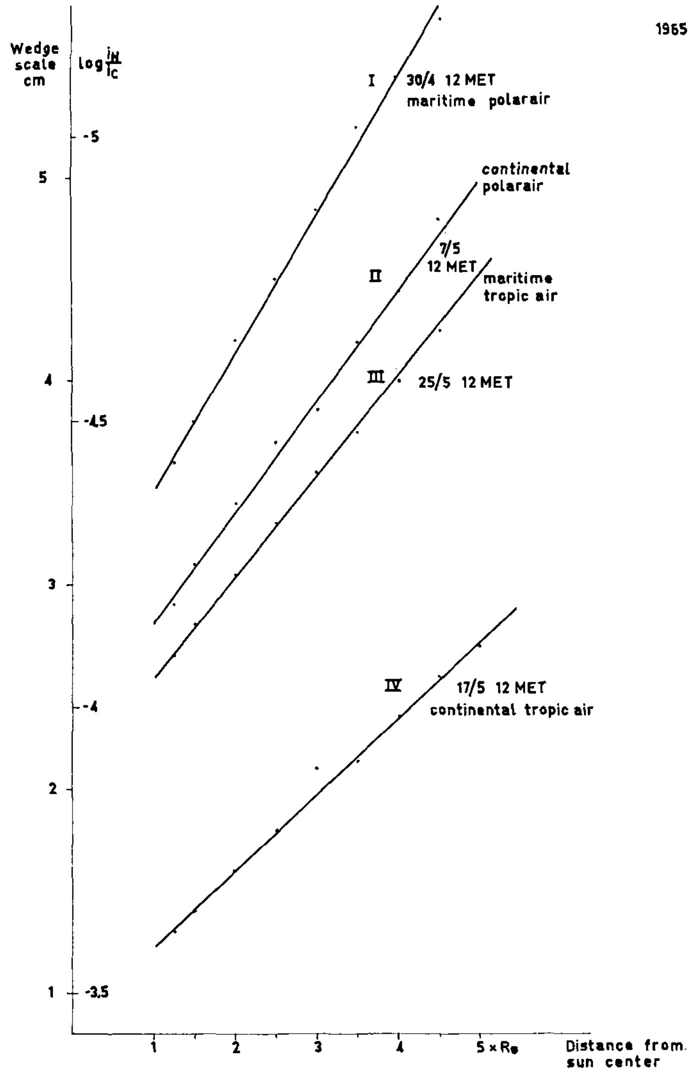

Fig. 7. Observed aureole intensity under various weather conditions (constant sun height).

about $\varphi = 60'$ and that the exponent varies with the specific air content, e.g. with the air mass. In any case it is possible to convert the exponential functions to linear curves and calculate graphically the function parameters k and l in the normal equation $\log i_H/i_c = kr + l$ (Fig. 7).

It is of interest in this connection to point out the existence of the obvious similarities concerning intensity gradient conditions which exist between the aureole and the sun corona. Though the scattering processes in the corona case are much more complicated and in certain respects are of a different nature, similar results have been obtained for the actual interval 4′–66′ using the principles of the observation method, sketched above (H. C. Hulst, 1947; S. Baumbach, 1938).

Results

1. The results from the main observation period are summarized in Fig. 7, in which measurements performed in different air masses during cloudless conditions are presented. According to the earlier discussions, the functions

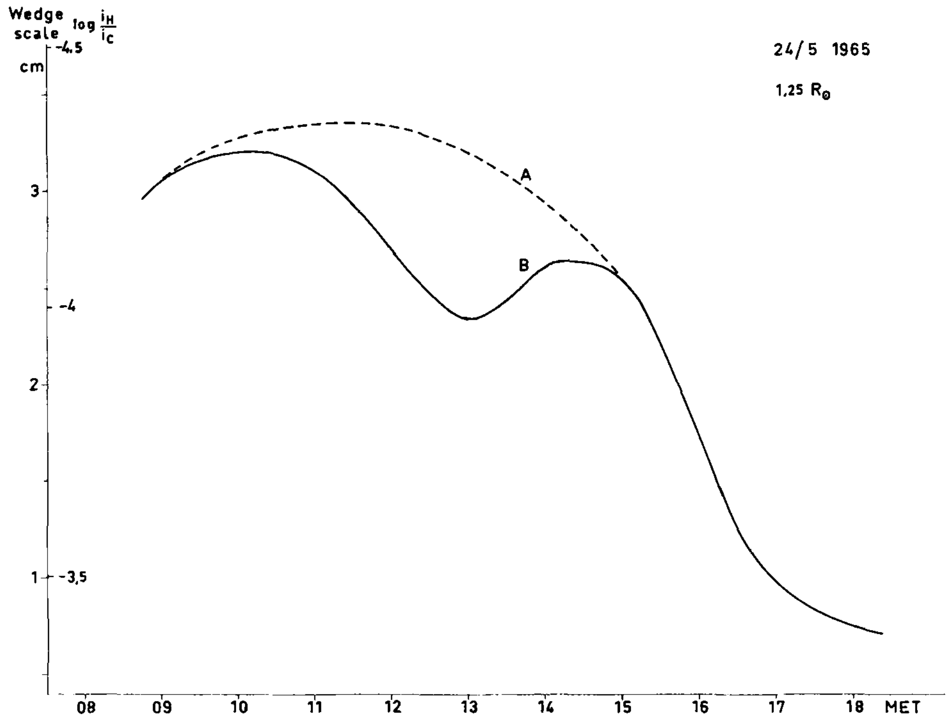

Fig. 8. Observed aureole intensity at a fixed angular distance and during a day with strong convection (curve *B*). Curve *A* shows the symmetrical intensity distribution around noon in an undisturbed atmosphere.

are assumed to be linear with the parameters k and l expressing the intensity gradient respectively the intensity level. The observations presented in Fig. 7 were made at about noon, e.g. approximately at the same sun height. The air mass types were deduced from weather analyses and representative aerological soundings. As can be seen in Fig. 7 there exists an evident difference in k and l between the four curves, each representing the distribution of intensity in an air mass with typical characteristic properties. The turbid tropical air masses show a definitely higher intensity and a slower aureole gradient out from the sun limb than the clean air masses from the arctic and polar regions.

2. The daily variation of the intensity at a constant distance from the sun limb is described in Fig. 8 for a representative cloudless calm day. There is obviously always a maximum (minimum in the curve B) in the intensity at 1–2 p.m. because of the daily convection, which increases the number of particles in the lower parts of the atmosphere. The corrected curve A shows a clear symmetry around noon and it can be transformed into a quasistraight line when reduced to constant sun height. This is a clear expression for the very stable weather conditions which prevailed on the actual day.

3. Finally, the intensity distribution concerning the vertical gradient has been examined during several days with stationary atmospheric conditions. The skyphotometer was brought by car and lift from sealevel up to the top of Monte Solaro (589 m) and back to the initial point in less than 1.5 hour. Observations were made at four fixed points along the road and for different distances from the sun limb as previously.

The results from one of these experiments are described in Fig. 9, in which the differences between the up- and downcurves depend mainly on the variation in the sun height with time. Taking a mean value between the two components in one pair of curves, one obtains a "constant-time-curve", which is sketched in Fig. 9. Because of the symmetry in time it is possible to determine the difference in intensity as a

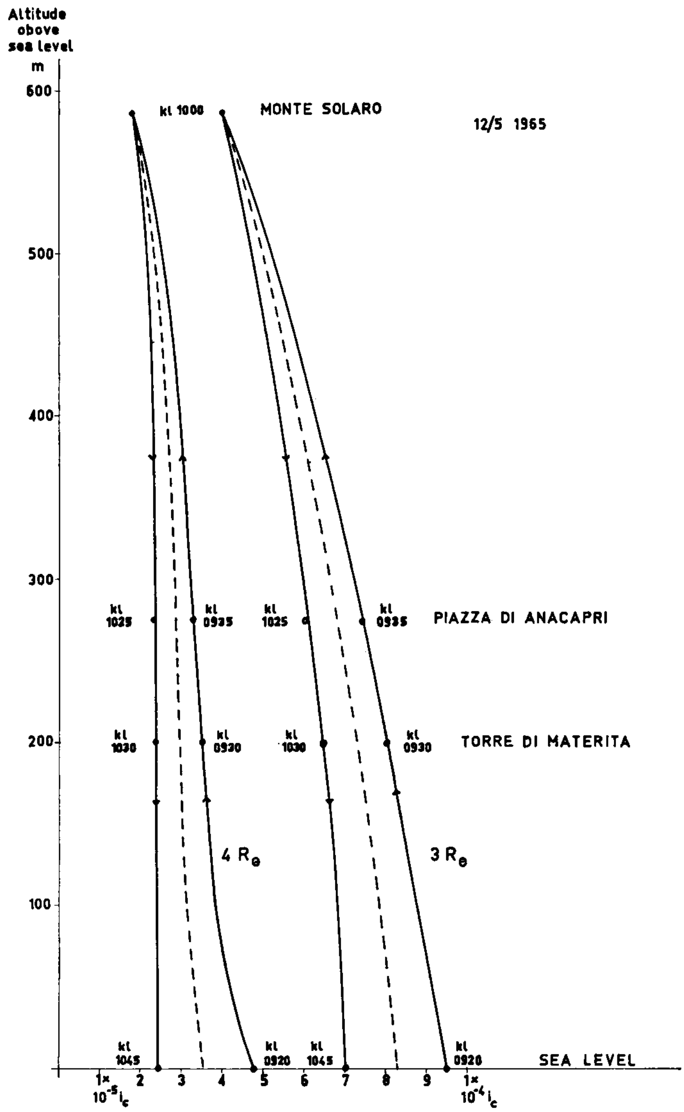

Fig. 9. Observed aureole intensity in altitude at different angular distances and under very stable weather conditions.

function of height. In this case the difference, which is caused mainly by the particle decrease, is for the lowest 600 m about $4 \times 10^{-4}\ i_c$ at a distance 3 $R_\odot$ from the sun limb.

Errors

F. Lindgren (1957) has shown earlier that the combined error from use of this method and instrumentation can be expressed as $\log i = \pm 0.04$. The errors arising from instrumental scattering in a conventional coronagraph have been estimated by Newkirk and Bohlin (1963) to be $5 \times 10^{-6}\ i_c$, which in the normal case is only a few per cent of the measured values.

Acknowledgement

The author wishes to express his great gratitude to Professor Yngve Öhman for his valuable advice and ideas in connection with the planning and performing of this study.

REFERENCES

Baumbach, S., 1938, Strahlung, Ergiebeigkeit und Elektronendichte der Sonnenkorona. *Veröffentlichungen der Universitäts-Sternwarte Kiel*, No. 22.

Evans, I. W., 1948, A photometer for measurement of sky brightness near the sun. *Journ. of the Optical Soc. of America. 38*, No. 12.

van de Hulst, H. C., 1948, Zodiacal light in the solar corona. *The Astrophysical Journal 105*, No. 3.

van de Hulst, H. C., 1957, *Light scattering by small particles*. John Wiley & Sons, London.

Lindgren, F., 1957, Time-intensity relations for H (Hα) and He (D_3) in some solar-prominences. *Stockholms Observatoriums Annaler. 19*, No 11.

Mie, G., 1908, Beiträge zur Optik trüber Medien, speziell kolloidaler Metallösungen. *Annalen der Physik, Vierte Folge 25.*

Newkirk, G. A., 1956, Photometry of the solar aureole. *Journ. of the Optical Soc. of America 46*, No. 12.

Newkirk, G. & Bohlin, D. 1963. Reduction of scattered light in the coronagraph. *Applied Optics 2.*

Penndorf, R., 1962, Angular mie scattering. *Journ. of the Optical Soc. of America 52*, No. 4.

Penndorf, R., 1962, Scattering and extinction coefficients for small absorbing and non-absorbing aerosols. *Journal of the Optical Soc. of America 52*, No. 8.

Unsöld, H., 1955, *Physik der Sternatmosfären.* Springer Verlag Berlin–Heidelberg–Göttingen.

Volz, F., 1954, Die Optik und Meteorologie der atmosfärische Trübung. *Berichte des Deutschen Wetterdienstes 2, no. 13.*

Öhman, Y., 1955, Coronagraphic work at moderate altitude above sea level. *Vistas in Astronoomy I*, A. Beer, ed. 750, London.

ФОТОМЕТРИЧЕСКОЕ ИЗУЧЕНИЕ СОЛНЕЧНОГО ОРЕОЛА ПРИ РАЗЛИЧНЫХ ПОГОДНЫХ УСЛОВИЯХ

С помощью коронографа и визуального фотометра для исследования небесного свода, основанного на принципе коронографа, исследуется интенсивность солнечного ореола в интервале угловых расстояний 4–66 от солнечного лимба. Результаты показывают, что существует хорошее согласие между типами превалирующих воздушных масс и характеристиками измеряемой интенсивности. Изучается и обсуждается изменение интенсивности с высотой и со временем.